

## Supporting Information

### **Ab Initio RAFT Emulsion Polymerization mediated by Small Cationic RAFT Agents to Form Polymers with Low Molar Mass Dispersity**

Sarah J. Stace,<sup>a,b</sup> Jochen Vanderspikken,<sup>b,c</sup> Shaun C. Howard,<sup>b</sup> Guoxin Li,<sup>b</sup> Benjamin W. Muir,<sup>b</sup> Christopher M. Fellows,<sup>\*,a</sup> Daniel J. Keddie<sup>\*,a,d</sup> and Graeme Moad<sup>\*,b</sup>

<sup>a</sup> School of Science and Technology, University of New England, Armidale, NSW 2351, Australia

<sup>b</sup> CSIRO Manufacturing, Bag 10, Clayton South, VIC 3169, Australia

<sup>c</sup> School of Biology, Chemistry and Forensic Science, University of Wolverhampton, Wulfruna Street, Wolverhampton West Midlands WV1 1LY, United Kingdom

## Experimental

### Materials

RAFT agents, cyanomethyl methyl(pyridin-4-yl)carbamodithioate (**3**) (98%) and 2-cyanopropan-2-yl methyl(pyridin-4-yl)carbamodithioate (**7**); initiators, 4,4'-azobis(4-cyanopentanoic acid) (ACPA, >98%) and sodium persulfate (NaPS, >99%); monomers, styrene, butyl acrylate (BA), butyl methacrylate (BMA), methyl methacrylate (MMA), vinyl acetate (VAc), and vinyl benzoate (VBz); and reagents, methyl iodide (99%), sodium dodecyl sulfate (99%), and 4-toluenesulfonic acid monohydrate (98%) were obtained from Sigma-Aldrich and purity confirmed by <sup>1</sup>H NMR. Monomers were purified (freed from inhibitor) by passage through neutral alumina unless otherwise indicated.

### Instrumentation

Nuclear magnetic resonance (NMR) spectra were obtained with a Bruker Avance 400 (400 MHz for <sup>1</sup>H, 100 MHz for <sup>13</sup>C). High resolution mass spectra were obtained with a Thermo Scientific Q Exactive FTMS employing ASAP/APCI probes.

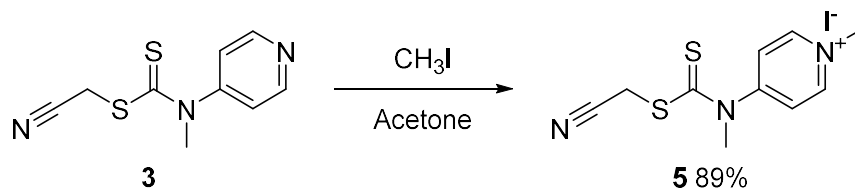
Gel permeation chromatography (GPC) was performed with a Waters Alliance 2695 Separations Module equipped with a 2414 differential refractometer, and a 2695 photodiode array detector. The columns used were 3×mixed C and 1×mixed E PLgel (each 7.5 mm×300 mm) from Agilent. Tetrahydrofuran (flow rate of 1.0 mL/min) was used as eluent at 35 °C. The columns were calibrated with narrow polydispersity polystyrene standards (Agilent). A third order polynomial was used to fit the log<sub>10</sub>M vs time calibration curve, which appeared approximately linear across the molar mass range 2 × 10<sup>2</sup> - 2 × 10<sup>6</sup> g mol<sup>-1</sup>.

Particle size distribution measurements were performed in a Zetasizer-Nano instrument (Malvern, UK). Particle size was measured in water directly on the latex and subsequently on the latex diluted to appropriately 10 mg/m l. with Milli-Q water. The analyses were performed at 25 °C. The data was analysed using the CONTIN algorithm.

For cryo-transmission electron microscopy (cryo-TEM) 300-mesh copper grids coated with perforated carbon film (Lacey carbon film: ProSciTech, Qld, Australia) were glow discharged in nitrogen to render them hydrophilic. A laboratory-built humidity-controlled vitrification system was used to prepare the samples for Cryo-TEM. Humidity was kept close to 80% for all experiments, and ambient temperature was 22°C. 4 µL aliquots of the sample were pipetted onto each grid prior to plunging. After 30 seconds adsorption time the grid was blotted manually using Whatman 541 filter paper, for 2 to 4 seconds. The grid was then plunged into liquid ethane cooled by liquid nitrogen. Frozen grids were stored in liquid nitrogen until required. The samples were examined using a Gatan 626 cryoholder (Gatan, Pleasanton, CA, USA) and Tecnai 12 Transmission Electron Microscope (FEI, Eindhoven, The Netherlands) at an operating voltage of 120 KV. At all times low dose procedures were followed, using

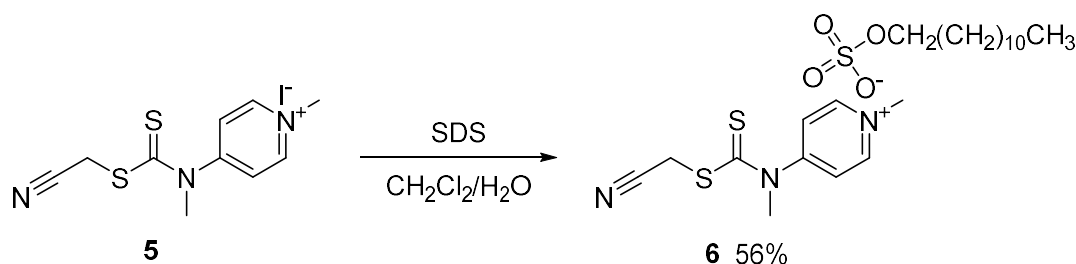
an electron dose of 8-10 electrons/Å<sup>2</sup> for all imaging. Images were recorded using a FEI Eagle 4k x 4k CCD camera at a range of magnifications.

### RAFT agent synthesis.



**Scheme S1.** Synthesis of 4-(((cyanomethyl)thio)carbonothioyl)(methyl)amino)-1-methylpyridin-1-ium iodide (**5**).

**4-(((cyanomethyl)thio)carbonothioyl)(methyl)amino)-1-methylpyridin-1-ium iodide (**5**).** Methyl iodide (1.3 mL, 20.79 mmol, 3 eq.) was added dropwise to a solution of **3** (1.5 g, 6.93 mmol) in acetone (25 mL) and the mixture was stirred for 24h. The precipitated solids were collected by filtration and washed with ice-cold acetone (100 mL). The quaternized RAFT agent **5** was obtained as a yellow solid (2.16 g, 6.2 mmol, 89%) and was characterized via NMR and mass spectrometry. <sup>1</sup>H-NMR (500 MHz, D<sub>2</sub>O): δ 3.78 (2H, s), 4.28 (1H, s), 4.34 (2H, s), 8.12 (1H, d), 8.82 (1H, d) (Figure S1). HRMS (ESI): HRMS (ESI): Calculated for C<sub>10</sub>H<sub>12</sub>N<sub>3</sub>S<sub>2</sub>: 238.0473 [M<sup>+</sup>]; found 238.0464, calculated for I: 126.9045 [M<sup>-</sup>]; found 126.9038.



**Scheme S2.** Synthesis of 4-(((cyanomethyl)thio)carbonothioyl)(methyl)amino)-1-methylpyridin-1-ium dodecyl sulfate (**6**).

**4-(((cyanomethyl)thio)carbonothioyl)(methyl)amino)-1-methylpyridin-1-ium dodecyl sulfate (**6**).** sodium dodecyl sulfate (1 eq., 288 mg, 1 mmol) and 20 mL DCM were added to a solution of **5** (350 mg, 1 mmol) in H<sub>2</sub>O (20 mL) and the mixture was stirred for 24h at ambient temperature. The mixture was transferred to an extraction flask and the organic layer separated. The residue after rotary evaporation was redissolved in 50 mL 10 v/v% DMSO/water and freeze-dried. The quaternized RAFT agent **6** was obtained as an orange solid (264 mg, 0.56 mmol, 56%) and was characterized via NMR and mass spectrometry. <sup>1</sup>H-NMR (500 MHz, CDCl<sub>3</sub>): 0.88 (3H, t), 1.29 (18H, m), 1.64 (2H, m), 3.87 (3H, s), 3.96 (2H, t, J=7 Hz), 4.14 (2H, s), 4.51 (3H, s), 8.07 (2H, d), 9.01 (2H, d) (Figure S2). HRMS (ESI): calculated for C<sub>10</sub>H<sub>12</sub>N<sub>3</sub>S<sub>2</sub>: 238.0473 [M<sup>+</sup>]; found 238.0466, calculated for C<sub>12</sub>H<sub>25</sub>O<sub>4</sub>S: 265.1474 [M<sup>-</sup>]; found 265.1477.

### $^1\text{H}$ NMR spectra of synthesized RAFT agents

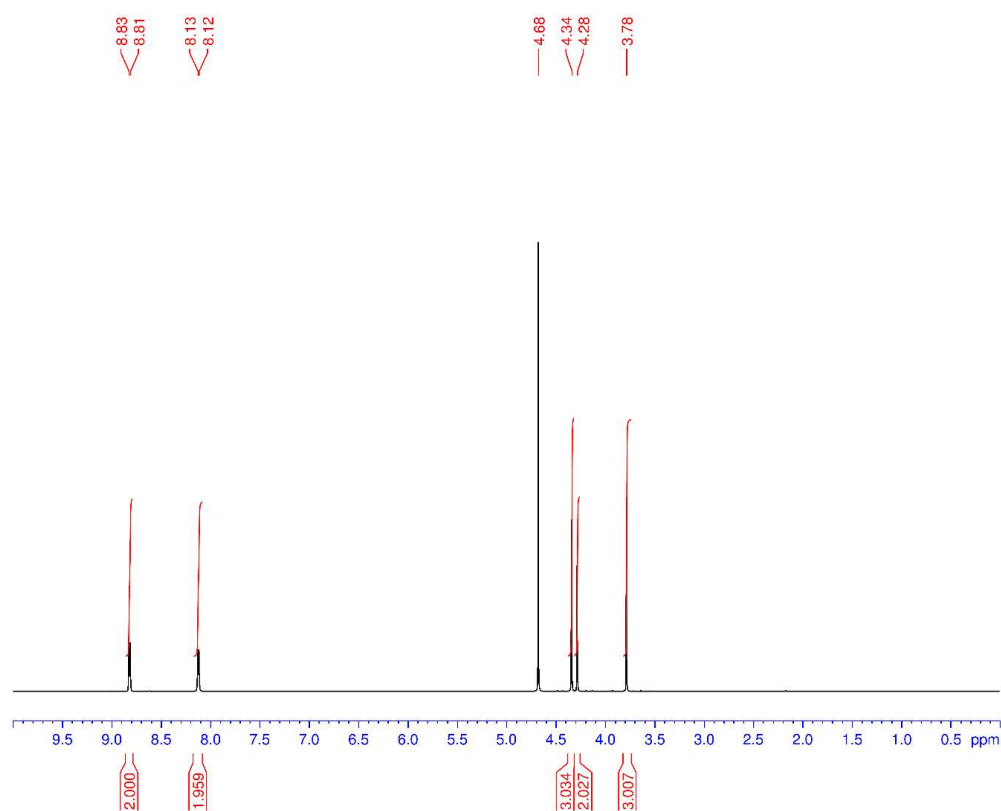


**Figure S1:**  $^1\text{H}$  NMR (D<sub>2</sub>O) of 4-(((cyanomethyl)thio)carbonothioyl)(methyl)amino)-1-methylpyridin-1-ium iodide (5).

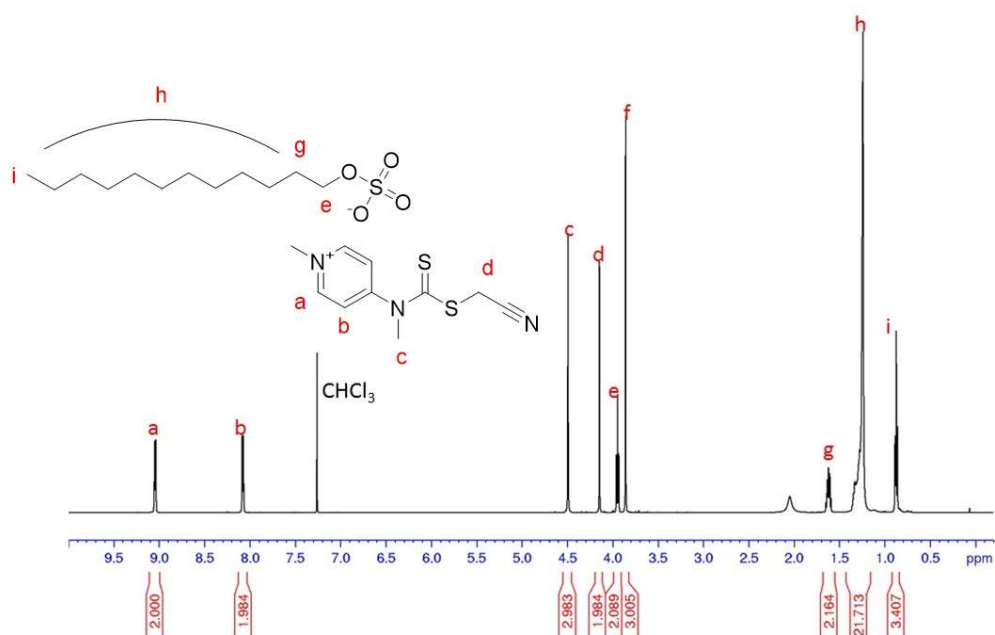


**Figure S2:**  $^1\text{H}$  NMR (CDCl<sub>3</sub>) of 4-(((cyanomethyl)thio)carbonothioyl)(methyl)amino)-1-methylpyridin-1-ium dodecylsulfate (6).

## Polymerization procedure for Schlenk flask experiments

**Initial experiments with cyanomethyl methyl(pyridin-4-yl)carbamdithioate (3) and with NaPS initiator** (Table 1, entry 1 and Table 2). The following procedure is typical. Styrene (3.75 g, 36 mmol), **3** (34.65 mg, 0.155 mmol), TsOH.H<sub>2</sub>O (29.5 mg, 0.155 mmol), SDS (43.7 mg, 1.51 mmol), distilled water (8.75 g) were combined in a Schlenk tube and an emulsion obtained by stirring overnight (~16 h). NaPS (3.07 mg, 1.28 × 10<sup>-5</sup> mmol) was added and the reaction solution degassed under vacuum. N<sub>2</sub> was bubbled through the emulsion for 20 minutes before it was heated and stirred for 5 hrs at 70 °C. Polymerization was quenched by the addition of 0.04 g MEHQ. The latex was freed of surfactant by dialysis. SEC characterisation was performed on polymer left after evaporation of water.

Note that NaPS is hydrolytically unstable and to be effective must be added just before polymerization.

Experiments with BA, MMA and BMA were carried out under similar conditions but with reaction times as given in Table 3 of the main document.

Experiments with VAc and VBz were carried out under similar conditions but without TsOH and with reaction times as given in Table 3 of the main document.

**Further experiments with 3 and those with ACPA initiator** (Table 1, entry 2). The following procedure is typical. Styrene (3.1 mL, 27 mmol), **3** (25.6 mg, 0.102 mmol), TsOH.H<sub>2</sub>O (19.4 mg, 0.102 mmol), SDS (43.3 mg, 0.15mmol) and ACPA (28.6 mg, 0.102 mmol) were combined in a Schlenk flask which was deoxygenated by sparging with Ar. Degassed water (10 mL, degassed by sparging with N<sub>2</sub> for 30 min) was then syringed into the Schlenk flask and the mixture was again sparged with Ar. The contents of the Schlenk flask were vigorously stirred for 24h to obtain an emulsion. The emulsion was heated to 70 °C under Ar. In some experiments, the conversion was followed by NMR by taking small aliquots that were extracted with CDCl<sub>3</sub>.

**Experiments with 4-(((cyanomethyl)thio)carbonothioyl)(methyl)amino)-1-methylpyridin-1-ium iodide (5) or 4-(((cyanomethyl)thio)carbonothioyl)(methyl)amino)-1-methylpyridin-1-ium dodecyl sulfate (6).** The following procedure is typical. Styrene (3.1 mL, 27 mmol), **3** (37.2 mg, 0.102 mmol), SDS (43.3 mg, 0.15 mmol) and ACPA (28.6 mg, 0.102 mmol) were combined in a Schlenk flask, sparged with Ar and sealed. Degassed water (10 mL) was then syringed into the Schlenk flask and the mixture was degassed again by sparging with Ar. The contents of the Schlenk flask were vigorously stirred for 24h to obtain an emulsion. The emulsion was heated to 70 °C under Ar.

## Bulk thermal polymerization of styrene with 5 at 110 °C

The procedure used has been described previously.<sup>1</sup> A stock solution comprising **5** (73.4 mg 0.146 mmol) in styrene (4.55 g, 5 mL, 43.69 mmol) was prepared. A reddish-black deposit was observed to have formed at the bottom of the ampoule after 1h. The <sup>1</sup>H NMR (Figure S3) indicates a loss of most signals associated with the RAFT agent (e.g., pyridine H at 8.88 and 8.03 ppm). The results of the experiments are summarized in Table S1 and Figure S3.

**Table S1.** Conversion and molar mass data for bulk thermal polymerization of styrene with **5** at 110 °C.

Time	Sty conversion <sup>a</sup>	RAFT agent <sup>a</sup>	$M_n^{\text{th } b}$	$M_n$	$\bar{D}$
1	<1	71	-	-	-
4	3	100	1560	16700	1.38
16	33	100	10200	50100	1.77

<sup>a</sup> determined by <sup>1</sup>H NMR (Figure S3). <sup>b</sup> Theoretical molar mass ( $M_n^{\text{th}}$ ) calculated using equation 3

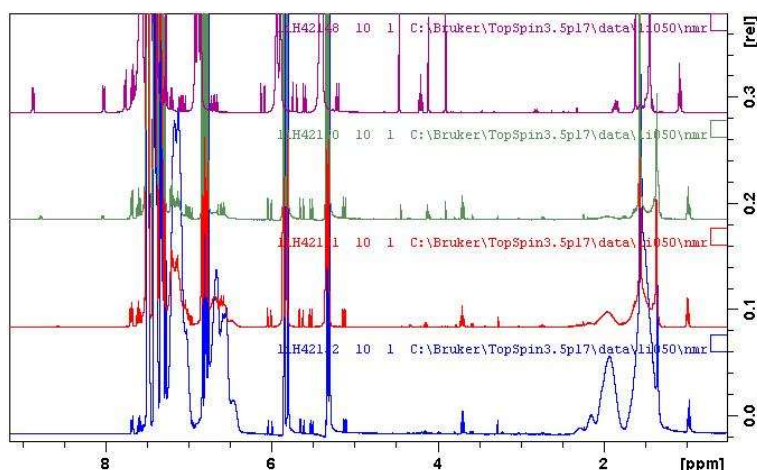


**Figure S3:** <sup>1</sup>H NMR spectra of polymerization mixture for bulk thermal polymerization of styrene with **5**. From top to bottom  $t=0$ , 1 h, 4 h, and 16 h. Monomer conversion was determined from the integration of signals due to olefinic H. RAFT agent conversion was determined for integration of signals for the pyridine H (8.88 and 8.03 ppm) relative to that for the dodecyl CH<sub>3</sub> (0.97 ppm).

### D<sub>2</sub>O/toluene-*d*<sub>8</sub> partition experiments

The partitioning of the RAFT agents **4**, **5**, and **6** between D<sub>2</sub>O and toluene-*d*<sub>8</sub> was qualitatively established as follows.

The non-protonated RAFT agent **1** was insoluble in D<sub>2</sub>O and fully soluble in toluene-*d*<sub>8</sub>.

RAFT agent **3** (11.1 mg) was placed in a 4 mL vial and 1 mL of each D<sub>2</sub>O and toluene-*d*<sub>8</sub> was added. 4-toluenesulfonic acid in the aqueous phase immediately becomes yellow consistent with the presence of protonated RAFT agent **4**. RAFT agent was not detectable in the toluene-*d*<sub>8</sub> phase by <sup>1</sup>H NMR but was present in the D<sub>2</sub>O phase.

The iodide salt of quaternized RAFT agent **5** was fully soluble in D<sub>2</sub>O. The dodecylsulfate salt of quaternized RAFT agent (**6**) was insoluble in D<sub>2</sub>O (none detectable by NMR) and fully soluble in toluene-*d*<sub>8</sub>.

RAFT agent **5** (23 mg) was placed in a 4 mL vial and 1 mL of toluene-*d*<sub>8</sub> was added to form a yellow solution. D<sub>2</sub>O was added and the mixture was vigorously shaken for 30 min forming an emulsion. The phases separated on standing. RAFT agent was not detectable in the colourless D<sub>2</sub>O phase by <sup>1</sup>H NMR.

### Results of Schlenk Flask Experiments with cyanomethyl methyl(pyridin-4-yl)carbamodithioate (**3**).

Initial experiments were performed with NaPS initiator, which was added immediately before heating the reaction mixture to polymerization temperature. Molar mass showed a trend to increase with monomer conversion but were generally higher than that expected for the monomer conversion and do not pass through the origin. This may indicate some consumption of RAFT agent through reaction with NaPS.

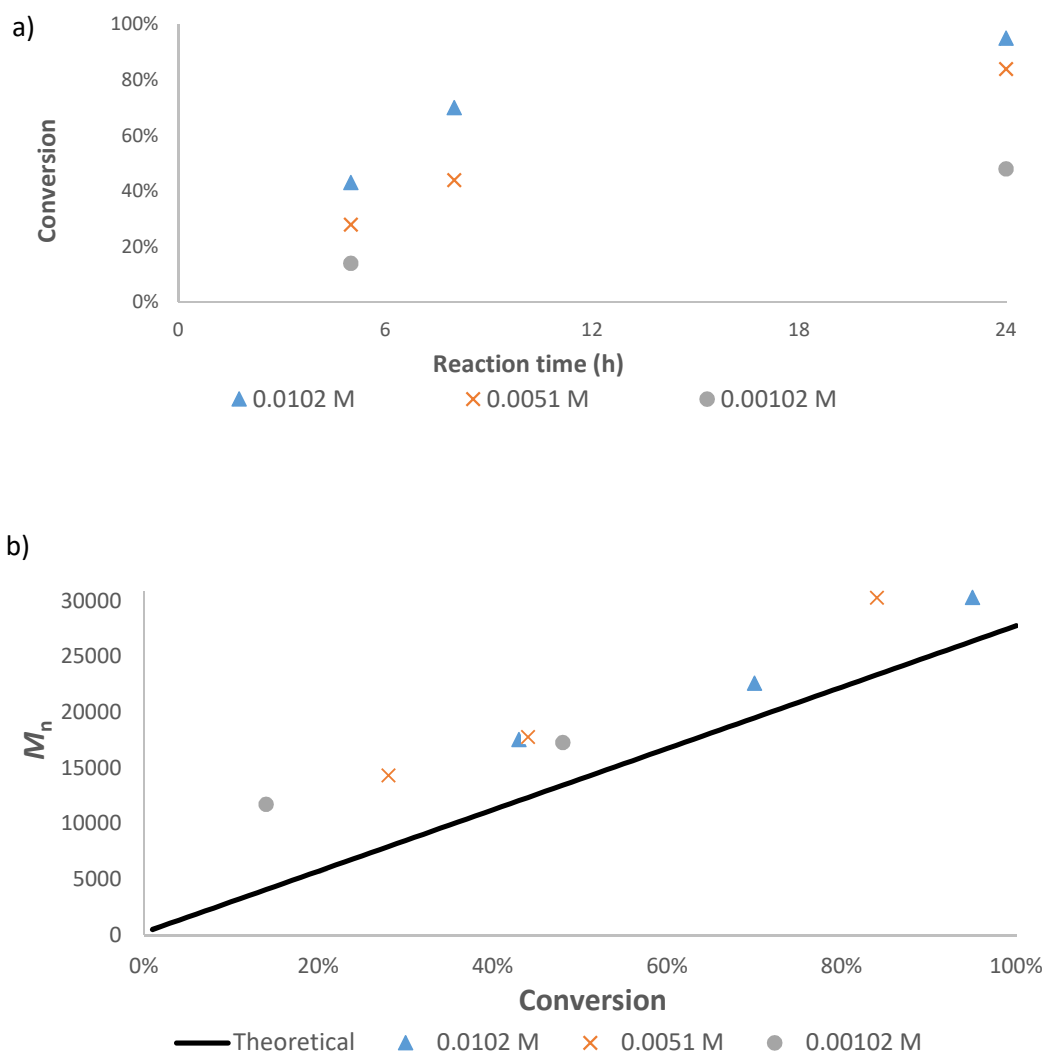


**Figure S4.** (a) Dependence of monomer conversion on reaction time and initiator concentration and (b) dependence of  $M_n$  on monomer conversion for *ab initio* emulsion polymerization of styrene with NaPS initiator concentrations as indicated and for 2.7 M styrene, 0.0102 M **3**, 0.0102 M TsOH, in 10 mL H<sub>2</sub>O at 70 °C. The solid line represents the theoretical molar mass ( $M_n^{\text{th}}$ ) that was calculated using equation 3.

In subsequent experiments with ACPA initiator the  $M_n$  was in accord with expectation based on the monomer conversion (refer Table S2, Figure S5 and Table S3). It was possible to add the initiator with other reagents (before degassing and forming the emulsion). It was still necessary to use a large amount of initiator to achieve a reasonable initiation rate, which is attributed to the very low initiator

efficiency of ACPA. Calculated initiator efficiencies based on the molar mass obtained (equation 4) were close to zero.

**Table S2.** *Ab initio* emulsion polymerization of styrene performed with the protonated RAFT agent **4** and different reaction times and/or ACPA initiator concentrations. <sup>a</sup>

Experiment	Time (h)	[ACPA]	$M_n^{\text{th}b}$ g mol <sup>-1</sup>	$M_n$	$\mathcal{D}$	Conv. (%)	$L^c$	$f^d$
1	8	0.0051	12100	14400	1.45	43	1.20	-0.32
2	8	0.0051	12600	15200	1.47	45	1.21	-0.33
3	8	0.0102	17000	16800	1.40	61	0.99	0.01
4	8	0.0102	16700	17000	1.39	60	1.02	-0.01
5	24	0.0102	26400	26400	1.40	95	1.00	-0.00

<sup>a</sup> 2.7 M styrene, 0.0102 M **3**, 0.0102 M TsOH, in 10 mL H<sub>2</sub>O at 70 °C. <sup>b</sup> Theoretical molar mass ( $M_n^{\text{th}}$ ) calculated using equation 3. <sup>c</sup> Fraction of living chains ( $L$ ) calculated using equation 6. <sup>d</sup> Initiator efficiency ( $f$ ) calculated using equation 4.

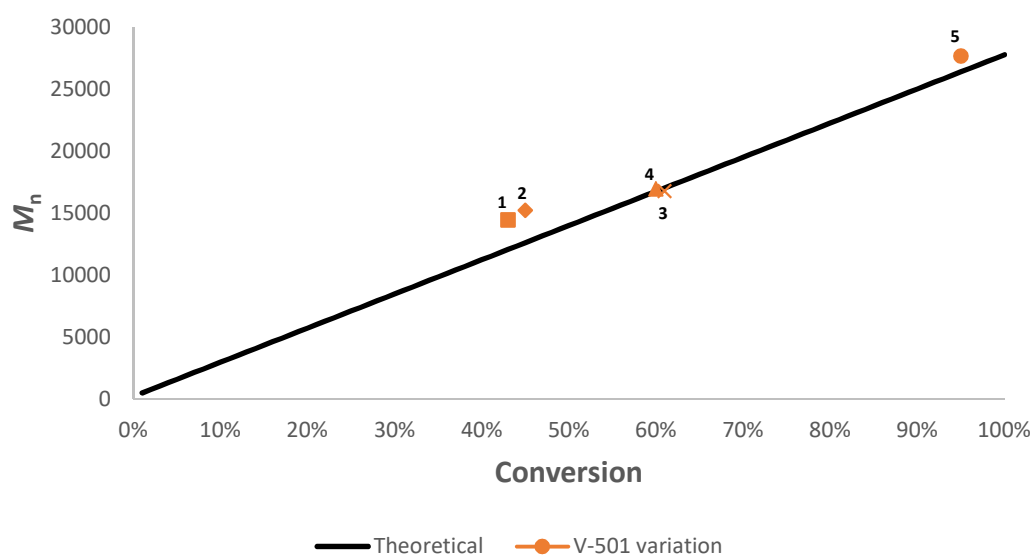


**Figure S5.** Dependence of  $M_n$  on monomer conversion observed for *ab initio* emulsion polymerization of styrene with different ACPA (V501) initiator concentrations and/or reaction times. Refer Table S2. Solid line represents the theoretical  $M_n$  as a function of conversion.

**Table S3.** *Ab initio* emulsion polymerization of styrene using the protonated RAFT agent **4**. Effect of surfactant (SDS) concentration. <sup>a</sup>

Time h	[SDS]	$M_n^{\text{th}b}$ g mol <sup>-1</sup>	$M_n$	$\bar{D}$	Conv. %	$D_p^*c$ nm
24	0.0075	26200	27700	1.4	95	93.67
24	0.0100	25300	25200	1.29	92	44.24
24	0.0150	25100	25400	1.32	91	60.20

<sup>a</sup> 2.7 M styrene, 0.0102 M **3**, 0.0102 M TsOH, 0.0102 M ACPA in 10 mL H<sub>2</sub>O at 70 °C. <sup>b</sup> Theoretical molar mass ( $M_n^{\text{th}}$ ) calculated using equation 3. <sup>c</sup>  $D_p^*$  is the particle diameter at the peak intensity maximum.

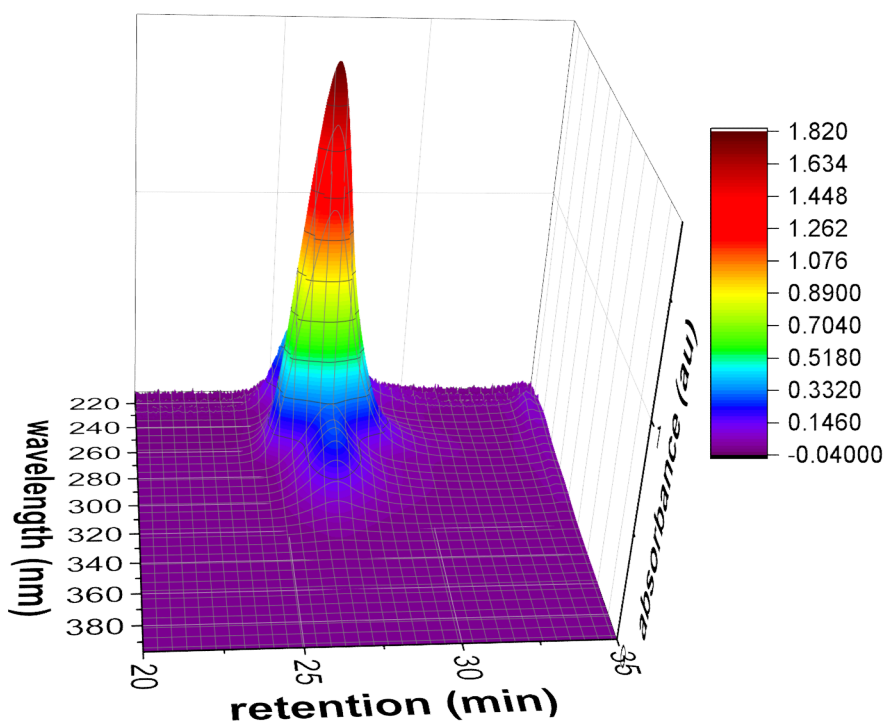


**Figure S6.** 3D plot of diode array (210-395 nm) data for GPC trace showing monomodal molar mass distribution observed for *ab initio* emulsion polymerizations of styrene using the protonated RAFT agent **4**. Sample corresponds Table S3, entry 3 and is typical for RAFT polymerization with RAFT agent **4** and ACPA initiator. The UV spectrum is consistent with the deprotonated end group **1**.

Particle size determination for the emulsions proved problematic. DLS for the emulsions show the dominant particle size as 30-100 nm, with some micellar or single chain species with size 5-10 nm, and a few larger particles > 1 microns (e.g. Figure S8). However, on dilution or after dialysis the particle sizes appeared to shift in most cases to ~ 200-500 nm. CryoTEM particle sizes (e.g. Figure S8) were generally consistent with this.

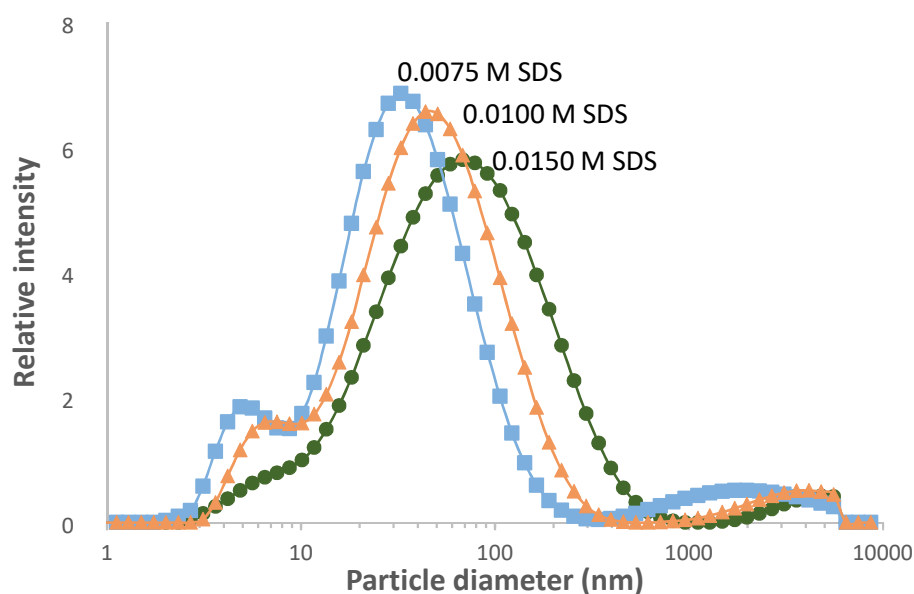


**Figure S7.** DLS measurements of the sols obtained from experiments with different SDS levels. Other characterization data appears in Table S3. Measured on a Malvern Zetasizer Nanoseries.

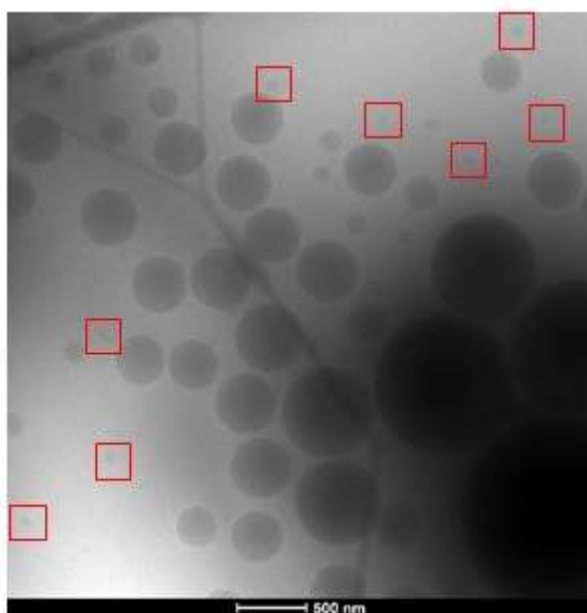


**Figure S8.** Cryo-TEM image of particles that shows several sized around 1  $\mu\text{m}$  and most particles with sizes between 250 and 500 nm. The red boxes indicate some particles with diameter between 70-90 nm, which DLS would indicate is the dominant particle size.

### Theoretical molar mass and fraction of living chains

Theoretical molar mass ( $M_n^{\text{th}}$ ) in RAFT polymerization can be evaluated from the following expression (equation 1).<sup>2</sup>

$$M_n^{\text{th}} = \frac{[M]_0 - [M]_t}{[T]_0 + df([I]_0 - [I]_t)} m_M + m_T \quad 1$$

where  $m_M$  and  $m_T$  are the molecular masses of the monomer (M) and the RAFT agent (T) respectively,  $d$  is the number of chains produced in a radical-radical termination event ( $d$  is typically taken as 1.0 in polymerization of St and other monosubstituted monomers) and  $f$  is the initiator efficiency.

If the concentration of initiator cannot be measured directly, it can often be calculated using equation 2.

$$[I]_0 - [I]_t = [I]_0(1 - e^{-k_d t}). \quad 2$$

Where  $k_d$  is the initiator decomposition rate constant under the reaction conditions. The use of this expression for KPS at pH 4 is considered unreliable as the values of  $k_d$  and  $f$  are not well defined because of the poor hydrolytic stability of KPS.

For values of  $M_n^{\text{th}}$  given in the paper, the contribution of initiator-derived chain was not considered and  $M_n^{\text{th}}$  was calculated using equation 3.<sup>2</sup>

$$M_n^{\text{th}} = \frac{[M]_0 - [M]_t}{[T]_0} m_M + m_T \quad 3$$

Given  $k_d$ , equations 1 can be rearranged to provide an estimate of the initiator efficiency for the experimentally observed  $M_n$ .

$$f = \frac{\frac{[M]_0 - [M]_t}{M_n - m_T} m_M - [T]_0}{d([I]_0 - [I]_t)}}{\frac{[M]_0 - [M]_t}{M_n - m_T} m_M - [T]_0} d[I]_0(1 - e^{-k_d t})} \quad 4$$

We have recently determined  $k_d$  for aqueous solution as follows.<sup>3</sup>

$k_d$  for racemic ACPA is  $4.76 \times 10^{15} \exp(-132200/(8.3144 T)) \text{ s}^{-1} \Rightarrow k_d(70^\circ\text{C}) 3.58 \times 10^{-5} \text{ s}^{-1}$ .

$k_d$  for *meso* ACPA is  $2.98 \times 10^{15} \exp(-131700/(8.3144 T)) \text{ s}^{-1} \Rightarrow k_d(70^\circ\text{C}) 2.67 \times 10^{-5} \text{ s}^{-1}$ .

The ACPA used in the present work was a (~1:1) mixture of stereoisomers.

This calculation suggests an initiator efficiency close to zero in the initial Schlenk flask experiments and ~20-50% in the Chemspeed experiments.

For the experiments with KPS where  $M_n$  is higher than theoretical even if initiator chains are not accounted for. This suggests that amount of RAFT agent is somewhat less than that used. This is indicative of side reactions (e.g., persulfate oxidation) removing the RAFT agent.

The fraction of living chains ( $L$ ) can be calculated using equation 5.<sup>2</sup> The uncertainty in initiator efficiency  $f$  makes this method unreliable in the present work.

$$L = \frac{[T]_0}{[T]_0 + df([I]_0 - [I]_t)} \quad 5$$

$L$  can also be calculated by comparing the found and theoretical molar mass as shown in equation 6.

$$L = \frac{(\bar{M}_n - m_{\text{RAFT}})[T]_0}{([M]_0 - [M]_t)m_M} \quad 6$$

Note that these expressions do not take into account loss of RAFT agent or other mechanisms for forming chains.

Values obtained using the above expressions appear in Tables S2, S9, S11 and S12.

### Results of Schlenk Flask Experiments with 4-(((cyanomethyl)thio)carbonothioyl)(methyl)amino)-1-methylpyridin-1-ium iodide (3).

Emulsion polymerization with the methyl iodide-quaternized RAFT agent **3** gave a low dispersity polymer with close to the anticipated  $M_n$  (Table S4) but GPC analysis shown that the molar mass distributions were distinctly bimodal (Figure S9, RI, Figure S10, photodiode array). The higher molar mass component and the sharp peak on the lower molar mass component do not possess the thiocarbonylthio chromophore (Figure S10).

**Table S4.** *Ab initio* emulsion polymerization of styrene using the methyl iodide quaternized RAFT agent **3**.<sup>a</sup>

[3] M	Time h	[styrene]/[3]	pH	$M_n^{\text{th}b}$ g mol <sup>-1</sup>	$M_n$	$\mathcal{D}$	Conv. (%)
0.0102	24	265	-	26116	23100	1.39	94
0.0065	24	415	4 <sup>c</sup>	43438	39900	1.30	100
0.0065	24	415	7 <sup>d</sup>	42142	217300	2.89	97

<sup>a</sup> 2.7 M styrene, 0.0102 M ACPA and 0.015 M SDS in 10 mL H<sub>2</sub>O at 70 °C. <sup>b</sup> Theoretical molar mass ( $M_n^{\text{th}}$ ) calculated using equation 3. Counterion of RAFT end-group not included in calculation. <sup>c</sup> Unbuffered pH 4. <sup>d</sup>Buffered to pH 7 using NaHCO<sub>3</sub>.

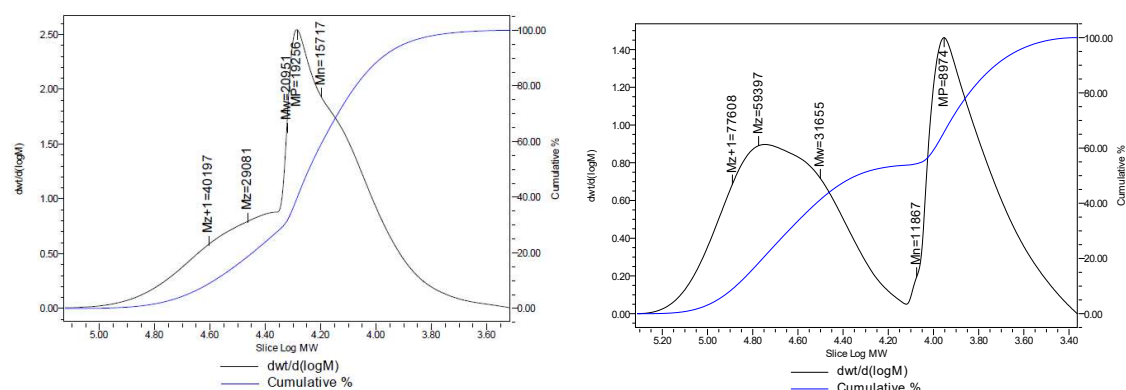


**Figure S9.** GPC traces with refractive index detection showing bimodal molar mass distributions observed for *ab initio* emulsion polymerizations of styrene using the methyl iodide quaternized RAFT agent **3**. Left: Table S4, entry 1. Right: Table S4, entry 2.

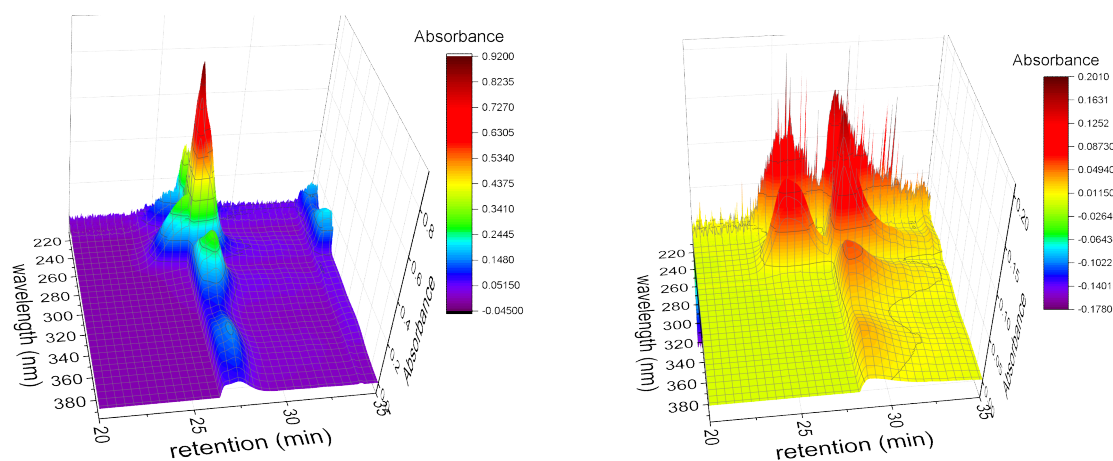
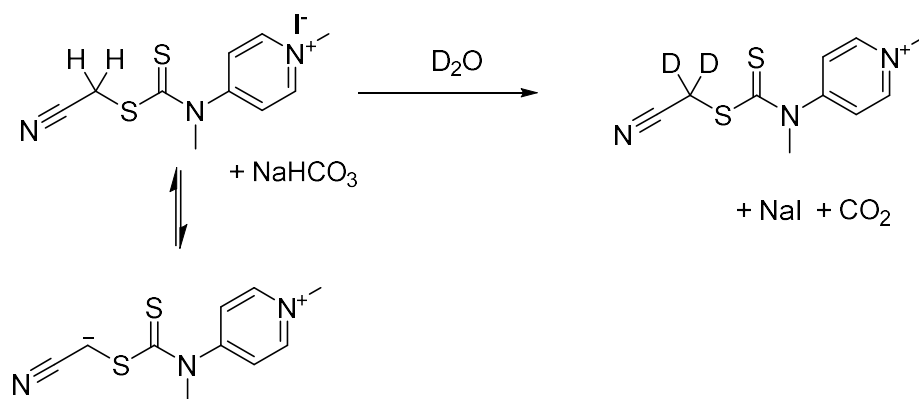


**Figure S10.** 3D plot of diode array (210-395 nm) data for GPC traces showing bimodal molar mass distributions observed for *ab initio* emulsion polymerizations of styrene using the methyl iodide quaternized RAFT agent **3**. Samples corresponds to left: Table S4, entry 1, and right: Table S4, entry 2.

It was hoped that use of the quaternized RAFT agent would enable polymerization at a higher pH more typical of those used in most conventional emulsion polymerization experiments in which SDS is used as a surfactant. However, RAFT polymerization carried out at pH 7 indicated no control (high molar mass product, broad dispersity) as shown in Table S4.

NMR experiments (Figure S11, pH 5.1; Figure S12, pH 8.4) show that the RAFT agent **3** undergoes rapid H-D exchange at pH > 7 (Scheme S3), though the RAFT agent appears otherwise unchanged.



**Scheme S3.** H-D exchange mechanism.

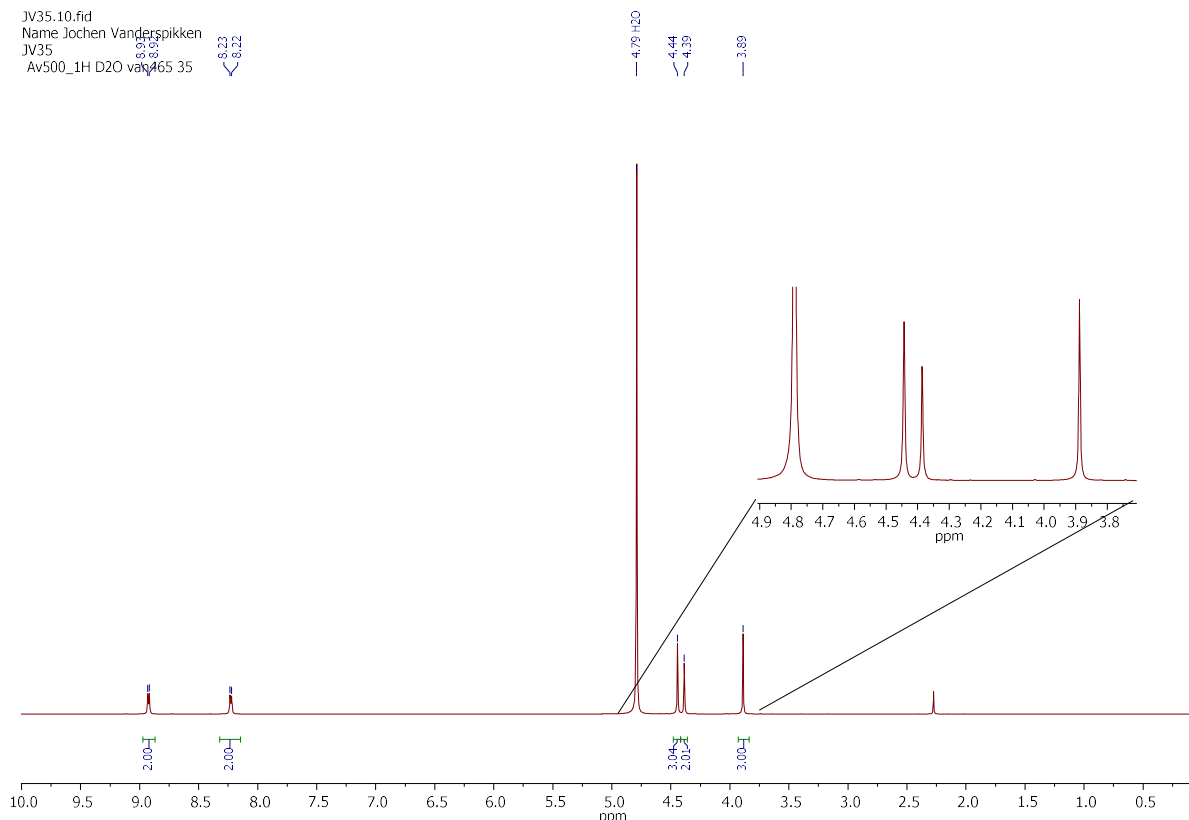


**Figure S11:** <sup>1</sup>H NMR (D<sub>2</sub>O) of 4-(((cyanomethyl)thio)carbonothioyl)(methylamino)-1-methylpyridin-1-ium iodide (**3**). pH of solution is 5.1.,

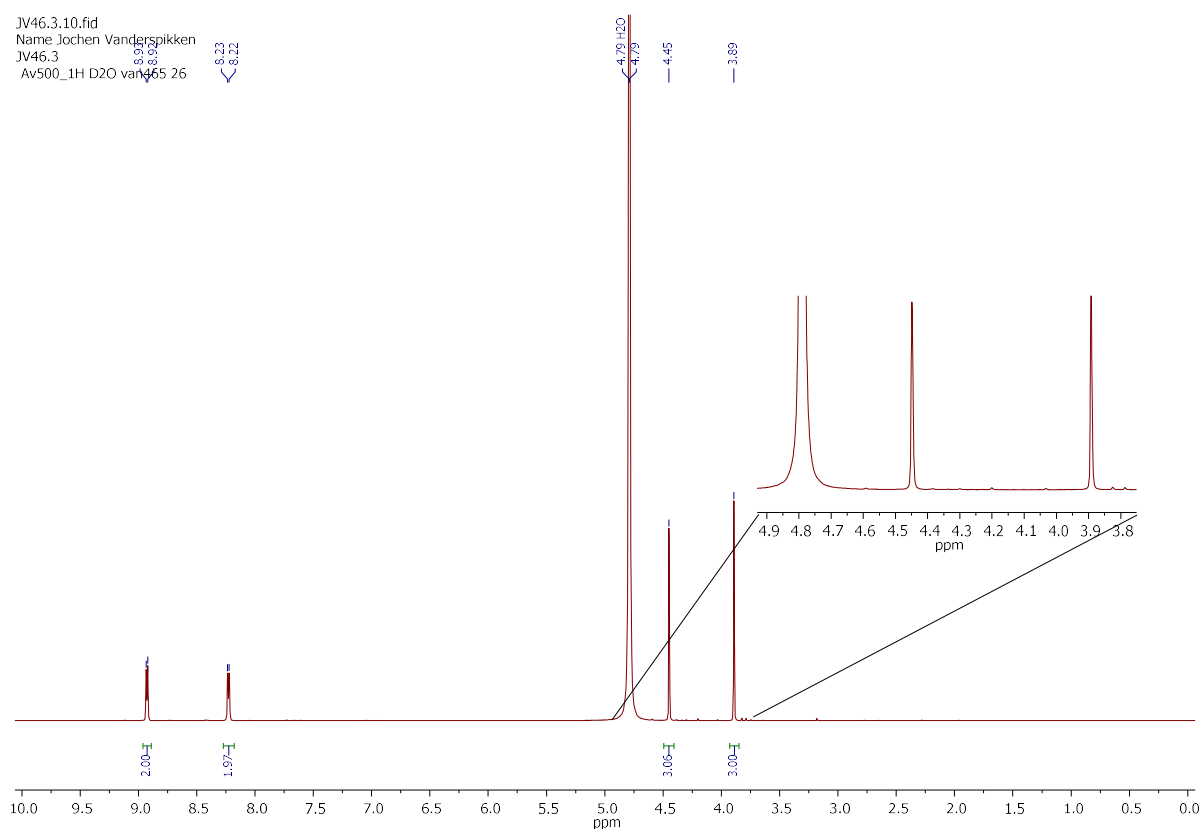


**Figure S12:**  $^1\text{H}$  NMR ( $\text{D}_2\text{O}$ ) of 4-(((cyanomethyl)thio)carbonothioyl)(methyl)amino)-1-methylpyridin-1-ium iodide (**3**) with pH adjusted to 8.4 with  $\text{NaHCO}_3$ ,

### Results of Schlenk Flask Experiments with 4-(((cyanomethyl)thio)carbonothioyl)(methyl)amino)-1-methylpyridin-1-ium dodecyl sulfate (**4**).

Experiments with **4** were conducted without addition of additional surfactant (Table S5). It was possible to combine the reagents and form an emulsion under the usual conditions. An initial experiment with the standard RAFT agent concentration (0.0102 M), while providing a low  $\bar{D}$  product, showed signs of latex instability with formation of a small amount of polystyrene “crust” or coagulum. A second experiment performed with the RAFT agent in similar concentration to that of SDS in previous experiments (0.015 M) gave a stable latex with no sign of “crust” and provided a lower  $\bar{D}$  product.

**Table S5.** *Ab initio* emulsion polymerization of styrene using the quaternized RAFT agent dodecyl sulfate salt.<sup>a</sup>

Time (h)	[ <b>4</b> ] (M)	$M_n^{\text{th},b}$ $\text{g mol}^{-1}$	$M_n$	$\bar{D}$	% Conv.	$D_p^*$ (nm)
21	0.0102	27492	39500	1.35	99	n.d.
24	0.015	18396	32100	1.27	97	24.24

<sup>a</sup> 2.7 M styrene, 0.0102 M ACPA in 10 mL  $\text{H}_2\text{O}$  at 70 °C. <sup>b</sup> Theoretical molar mass ( $M_n^{\text{th}}$ ) calculated using equation 3. Counterion of RAFT end-group not included in calculation.

The molar mass in the experiments with **4** is significantly higher than predicted. GPC analysis with the photodiode array detector shows that the polymer has largely lost the RAFT end group (Figure S13). The RAFT chromophore appears at long retention time (>32 min, low molar mass). However, this is insufficient to explain the discrepancy. It is possible that the RAFT agent was contaminated with SDS or residual solvent effectively meaning that a lower concentration than expected was used in these experiments.

Particle size distributions were similar in appearance to those obtained on emulsion polymerization with RAFT agents **2** and **3** and showed a similar dependence on dilution (Figure S14).

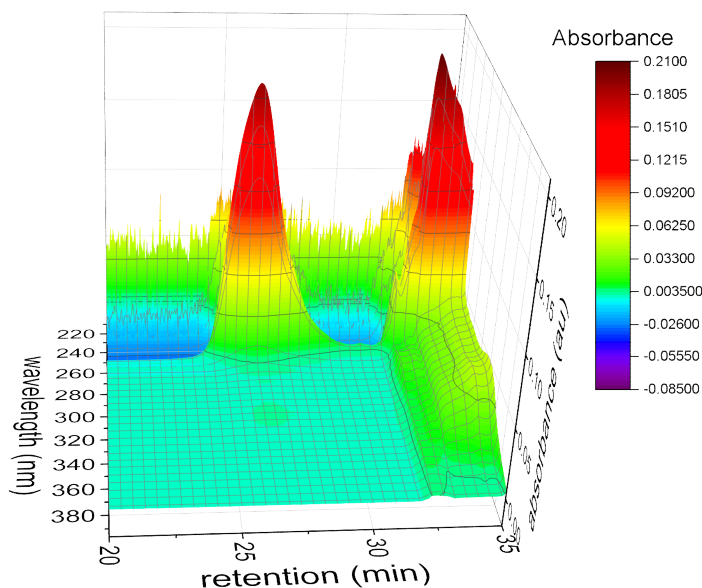


**Figure S13.** 3D plot of diode array (210-395 nm) data for GPC traces showing molar mass distribution observed for *ab initio* emulsion polymerizations of styrene using the quaternized RAFT agent **4**. Sample corresponds to that in Table S5, entry 2.

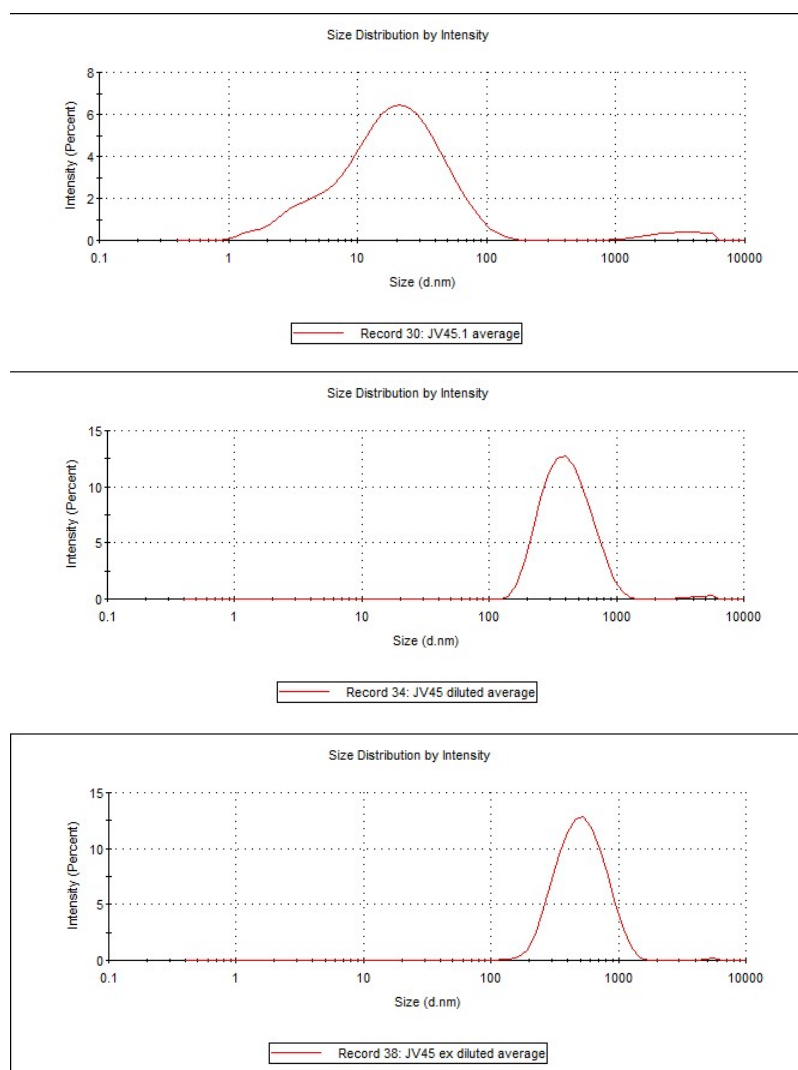


**Figure S14.** DLS particle size distributions from top to bottom: latex, (b) sample diluted to ca 10 mg/mL with MilliQ® water (c) sample further diluted with MilliQ® water. Sample corresponds to that produced in Table S5, entry 2.

## Chemspeed experiments

A Chemspeed Swing robot equipped with an ISYNTH reactor containing 48 individual reactors was used for all polymerisations. The ISYNTH reactor was fitted with 8 mL disposable glass vials from (Chemspeed Technologies Pty Ltd). The solid components (cyanomethyl methyl(pyridin-4-yl)carbamodithioate (**1**), ACPA, SDS) were manually weighed into the individual reaction vials while the stock solutions (TsOH, styrene, water) were dispensed using the 4-Needle Head tool equipped with 2 x 1 mL and 2 x 10 mL syringes fitted with stainless steel septa piercing needles. Styrene was first purified by passage through a basic alumina column in order to remove the stabilizer. All solvent lines were primed with degassed water or DMF which was used for each rinsing step. Typical aspiration and dispense rates of the reagents were 2 mL/min and 5 mL/min respectively for the 1 mL syringes and 10 mL/min and 5 mL/min respectively for the 10 mL syringes. An airgap of 50  $\mu$ L and an extra volume of 50  $\mu$ L was used for all aspirations using the 4-Needle Head tool. The needles were rinsed after each reagent dispense step with a 3 mL inside and outside volume for the 1 mL syringes and a 5 mL inside and outside volume for the 10 mL syringes. The enclosed Chemspeed robotic deck was made inert by means of a constant nitrogen purge of >50 L/min to remove all oxygen with the extraction ports closed. Argon purged reagent vials were passed into the robot immediately after the completion of degassing using a transfer chamber with a vacuum set to 200 mbar to minimise any exposure to

oxygen. After addition of all reagents the ISYNTH lid was set to sealed (closed independent) for the polymerisations and was actively cooled to 4 °C. The ISYNTH reactor temperature was held at 20 °C for 14 hours with a specific shaking protocol designed to ensure a stable emulsion was produced. This involved vortexing the reactor vials at 800 and 600 rpm for cycles of 10 seconds and 13 minutes, respectively, over the 14 hours (a variety of shaking protocols were explored; omission of the high-speed vortexing cycle failed to produce a stable emulsion). After this time, the shaking cycle was continued while the reactors were heated to 70 °C (~ 5 min) to start polymerization and continued at 70 °C for another 24h. Details of the contents of the individual reactors were as follows (Table S6).

**Table S6.** Contents of reactor vials for Chemspeed experiments.

Chemspeed table		All values in mL					All values in g		
Experiment name	Vials Experiment vial	Stock solutions		Pure		Stock solution	Solids	RAFT	Initiator
		Q,RAFT	Styrene	Water	TsOH	SDS			
		1	2	3	4				
Column1	Column2	Column3	Column4	Column5	Column6	Column7	Column8		
JV50	1		1.2374	3.2000	0.8000	0.0173022	0.00911456	0.01435424	
JV50.1	2		1.2374	3.2800	0.7200	0.0173022	0.00911456	0.01435424	
JV50.2	3		1.2374	3.3600	0.6400	0.0173022	0.00911456	0.01435424	
JV50.3	4		1.2374	3.5200	0.4800	0.0173022	0.00911456	0.01435424	
JV50.4	5		1.2374	3.1200	0.8800	0.0173022	0.00911456	0.01435424	
JV50.5	6		1.2374	3.0400	0.9600	0.0173022	0.00911456	0.01435424	
JV51.1	7		1.2374	3.2000	0.8000	0.0173022	0.002858856	0.01435424	
JV51.2	8		1.2374	3.2000	0.8000	0.0173022	0.00911456	0.005717712	
JV51.3	9		1.2374	3.2000	0.8000	0.0173022	0.00911456	0.008576568	
JV51.4	10		1.2374	3.2000	0.8000	0.0173022	0.00911456	0.01429428	
JV51.5	11		1.2374	3.2000	0.8000	0.0173022	0.00911456	0.017153136	
JV51.6	12		1.2374	3.2000	0.8000	0.0173022	0.00911456	0.022870848	
JV52.1	13		1.2374	3.2000	0.8000	0.01038132	0.00911456	0.01435424	
JV52.2	14		1.2374	3.2000	0.8000	0.01384176	0.00911456	0.01435424	
JV52.3	15		1.2374	3.2000	0.8000	0.02076264	0.00911456	0.01435424	
JV52.4	16		1.2374	3.2000	0.8000	0.02422308	0.00911456	0.01435424	
JV52.5	17		1.2374	3.2000	0.8000	0.02768352	0.00911456	0.01435424	
JV52.6	18		1.2374	3.2000	0.8000	0.0346044	0.00911456	0.01435424	
JV53.1	19		0.9899	3.2000	0.8000	0.0173022	0.00911456	0.01435424	
JV53.2	20		0.7425	3.2000	0.8000	0.0173022	0.00911456	0.01435424	
JV53.3	21		0.4950	3.2000	0.8000	0.0173022	0.00911456	0.01435424	
JV53.4	22		1.4849	3.2000	0.8000	0.0173022	0.00911456	0.01435424	
JV53.5	23		1.7324	3.2000	0.8000	0.0173022	0.00911456	0.01435424	
JV54.1	24		1.2374	3.5200	0.4800	0.0173022	0.005466874	0.01435424	
JV54.2	25		1.2374	3.3600	0.6400	0.0173022	0.007289165	0.01435424	
JV54.3	26		1.2374	3.0400	0.9600	0.0173022	0.010933747	0.01435424	
JV54.4	27		1.2374	2.8000	1.2000	0.0173022	0.013667184	0.01435424	
JV55	28	0.8000	1.2374	3.2000		0.0173022		0.01435424	
JV55.1	29	0.8000	1.2374	3.2000		0.0173022		0.002858856	
JV55.2	30	0.8000	1.2374	3.2000		0.0173022		0.005717712	
JV55.3	31	0.8000	1.2374	3.2000		0.0173022		0.008576568	
JV55.4	32	0.8000	1.2374	3.2000		0.0173022		0.01429428	
JV55.5	33	0.8000	1.2374	3.2000		0.0173022		0.017153136	
JV55.6	34	0.8000	1.2374	3.2000		0.0173022		0.022870848	
JV56.1	35	0.8000	1.2374	3.2000		0.01038132		0.01435424	
JV56.2	36	0.8000	1.2374	3.2000		0.01384176		0.01435424	
JV56.3	37	0.8000	1.2374	3.2000		0.02076264		0.01435424	
JV56.4	38	0.8000	1.2374	3.2000		0.02422308		0.01435424	
JV56.5	39	0.8000	1.2374	3.2000		0.02768352		0.01435424	
JV56.6	40	0.8000	1.2374	3.2000		0.0346044		0.01435424	
JV57.1	41	0.8000	0.9899	3.2000		0.0173022		0.01435424	
JV57.2	42	0.8000	0.7425	3.2000		0.0173022		0.01435424	
JV57.3	43	0.8000	0.4950	3.2000		0.0173022		0.01435424	
JV57.4	44	0.8000	1.4849	3.2000		0.0173022		0.01435424	
JV57.5	45	0.8000	1.7324	3.2000		0.0173022		0.01435424	
JV58.1	46	0.4000	1.2374	3.6000		0.0173022		0.01435424	
JV58.2	47	1.2000	1.2374	2.8000		0.0173022		0.01435424	
JV58.3	48	1.6000	1.2374	2.4000		0.0173022		0.01435424	

RAFT = cyanomethyl methyl(pyridin-4-yl)carbamodithioate (**2**) which was transformed to **2** in reactor.

QRAFT = 4-(((cyanomethyl)thio)carbonothioyl)(methyl)amino)-1-methylpyridin-1-ium iodide (**3**). Initiator = ACPA.

## Chemspeed experiments with ((cyanomethyl)thio)carbonothioyl(methyl)amino)pyridin-1-ium toluenesulfonate (**2**).

For experiments with RAFT agent **2** (formed in situ from **1** and TsOH), the concentrations of TsOH, ACPA, SDS and styrene were varied independently, the concentrations of TsOH and cyanomethyl methyl(pyridin-4-yl)carbamodithioate concentration were varied in unison.

A reference experiment using the same reagent concentrations as a previous Schlenk flask experiment was conducted. This yielded a slightly higher conversion of 97% (vs 95%), higher  $\bar{D}$  1.48 (vs 1.40) and lower  $M_n$  22400 (vs 27700) (Table S7). It is unclear if differences reflect inaccuracies in dispensing precision or reaction conditions.

**Table S7.** Comparison of Chemspeed and Schlenk flask experiments

	[RAFT] M	[TsOH] M	[Initiator] M	[SDS] M	[Styrene] M	% Conv.	$M_n$	$\mathcal{D}$	$M_n^{\text{th}^a}$ g mol <sup>-1</sup>
Chemspeed	0.0102	0.0102	0.0102	0.015	2.7	97	22400	1.48	26700
Schlenck	0.0102	0.0102	0.0102	0.015	2.7	95	27700	1.40	26200

<sup>a</sup> Theoretical molar mass ( $M_n^{\text{th}}$ ) calculated using equation 3.

The TsOH concentration was varied to be 60, 80, 90, 110 and 120% of the concentration used in the reference experiment (Table S8). The TsOH concentration does not have a substantial influence on the conversion or the molar mass. Previous work for polymerizations in solution indicated that lowest dispersities could be obtained with stoichiometric acid.

**Table S8.** Effect of variation of the *p*-toluenesulfonic acid (TsOH) concentration<sup>a</sup>

[TsOH]	% Conversion	$M_n^{\text{th}^b}$ g mol <sup>-1</sup>	$M_n$	$\mathcal{D}$
0.00612	98	27200	23500	1.44
0.00816	98	27200	22900	1.40
0.00918	97	26700	23700	1.42
0.0102	97	26700	22400	1.48
0.01122	98	27200	23400	1.42
0.01224	97	27000	25500	1.45

<sup>a</sup> Other conditions same as for reference experiment (Table S7). <sup>b</sup> Theoretical molar mass ( $M_n^{\text{th}}$ ) calculated using equation 3.

The initiator concentration was varied to utilize 25, 50, 75, 110, 150 and 200% of the original initiator concentration (Table S9). It was expected that a lower initiator concentration would result in a lower conversion and therefore lower molar mass. Higher initiator concentrations should produce more initiator-derived chains more termination and therefore lower fraction of living chains, lower molar mass and higher dispersity. The lowest (0.00255 mol/l) initiator concentration results in only 46% conversion. Other initiator concentrations resulted in similar, close to full, conversion. The  $M_n$  value for 0.0051 ACPA is slightly higher and the  $\mathcal{D}$  slightly lower but all values might be considered to be the same within experimental error.

**Table S9.** Effect of variation of the initiator (ACPA) concentration <sup>a</sup>

[ACPA] M	% Conversion	$M_n^{\text{th } b}$ g mol <sup>-1</sup>	$M_n$	$\mathcal{D}$	$L^c$	$f^d$
0.00255	46	12900	13400	1.41	1.04	-0.15
0.0051	96	26700	29900	1.39	1.12	-0.25
0.00765	97	26900	24400	1.42	0.91	0.13
0.0102	97	26900	22400	1.48	0.83	0.19
0.01275	98	27200	22900	1.41	0.84	0.14
0.0153	98	27200	24500	1.43	0.90	0.07
0.0204	98	27200	20800	1.47	0.76	0.15

<sup>a</sup> Other conditions same as for reference experiment (Table S7). <sup>b</sup> Theoretical molar mass ( $M_n^{\text{th}}$ ) calculated using equation 3. <sup>c</sup> Fraction of living chains ( $L$ ) calculated using equation 6. <sup>d</sup> Initiator efficiency ( $f$ ) calculated using equation 4.

No clear trends can be seen in the values of  $M_n$  or  $\mathcal{D}$  as a function of [SDS] (Table S10). Particle size distributions for the reference experiment are similar to those seen in the Schlenk flask experiments. The main population appears centred at  $\sim 60$  nm. There are also “micellar species” at  $\sim 8$  nm and large aggregates with particle size  $> 1 \mu$ . At the highest SDS concentrations within the range explored, DLS particle sizes appear larger and a distinct broadening of the distribution is apparent (Figure S15). CryoTEM was not performed.

**Table S10.** Effect of variation of the surfactant (SDS) concentration <sup>a</sup>

SDS M	% Conversion	$M_n^{\text{th } b}$ g mol <sup>-1</sup>	$M_n$	$\mathcal{D}$	$D_p^*$ nm
0.009	97	27000	25700	1.42	113.8
0.012	98	27200	25500	1.47	86.64
0.018	98	27200	18100	1.42	83.18
0.015	97	27000	22400	1.48	99.17
0.021	98	27200	22900	1.41	83.52
0.024	98	27200	24900	1.46	146.9
0.03	98	27200	22000	1.54	199.7

<sup>a</sup> Other conditions same as for reference experiment (Table S7). <sup>b</sup> Theoretical molar mass ( $M_n^{\text{th}}$ ) calculated using equation 3.

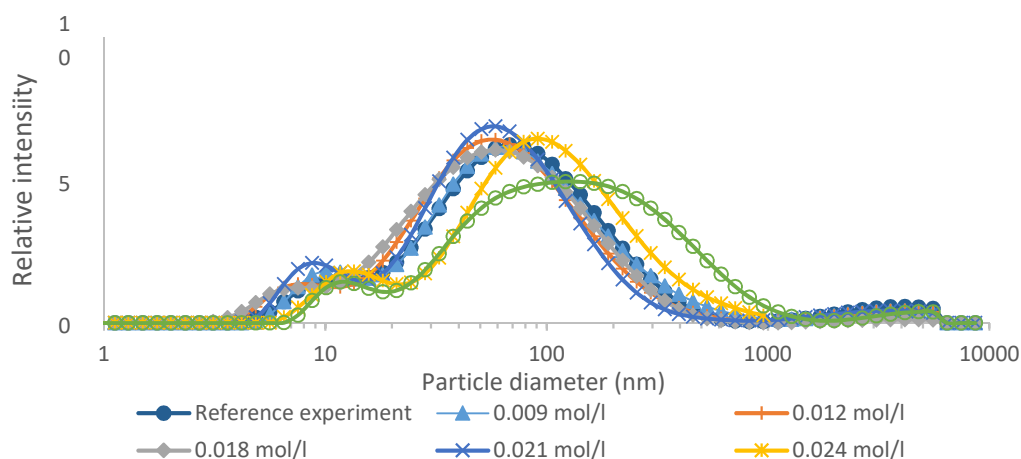


**Figure S15.** DLS measurement of the sols obtained as a function of [SDS] concentration. Measured on a Malvern Zetasizer Nanoseries.

Experiments with 40, 60, 80, 120 and 140% of the original styrene concentration were carried out (Table S11). Close to full conversion was seen in all experiments. The molar mass increases with increasing styrene concentration. Variation of the styrene concentration does not have a significant influence on the particle size or size distribution as measured by DLS.

**Table S11.** Effect of variation of the styrene concentration <sup>a</sup>

[Styrene] M	% Conversion	$M_n^{\text{th } b}$ g mol <sup>-1</sup>	$M_n$	$\mathcal{D}$	$D_p^*$ nm	$L^c$	$f^d$
1.08	99	11100	10200	1.45	122.90	0.92	0.09
1.62	98	16400	15000	1.42	117.10	0.91	0.09
2.16	98	21800	19900	1.44	87.79	0.91	0.09
2.70	97	26900	22400	1.48	99.17	0.83	0.19
3.24	97	32300	29800	1.47	93.63	0.92	0.08
3.78	98	38000	31500	1.48	109.00	0.83	0.20

<sup>a</sup> Other conditions same as for reference experiment (Table S7). <sup>b</sup> Theoretical molar mass ( $M_n^{\text{th}}$ ) calculated using equation 3. <sup>c</sup> Fraction of living chains ( $L$ ) calculated using equation 6. <sup>d</sup> Initiator efficiency ( $f$ ) calculated using equation 4.

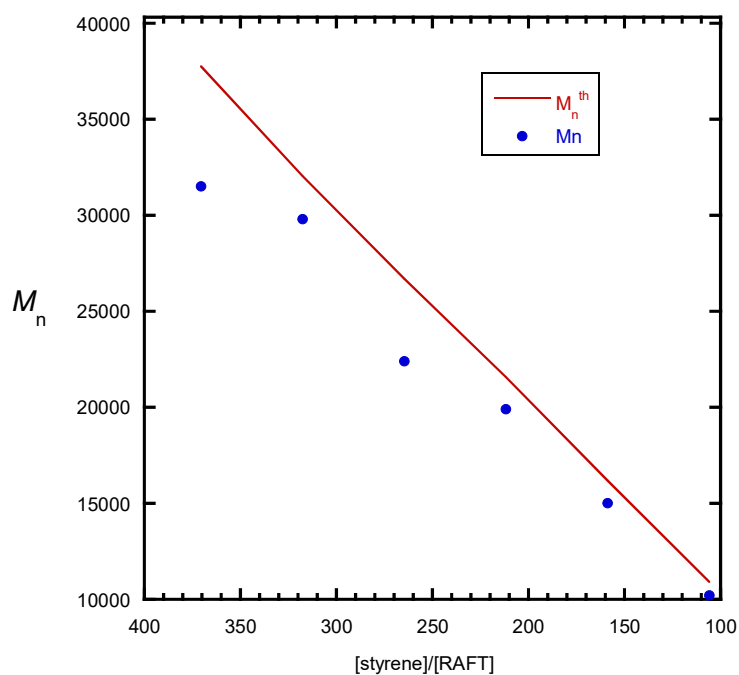


**Figure 16.** Theoretical and experimental  $M_n$  as a function of [styrene]/[1] for varying [styrene]. <sup>b</sup> Theoretical molar mass ( $M_n^{th}$ ) was calculated using equation 3.

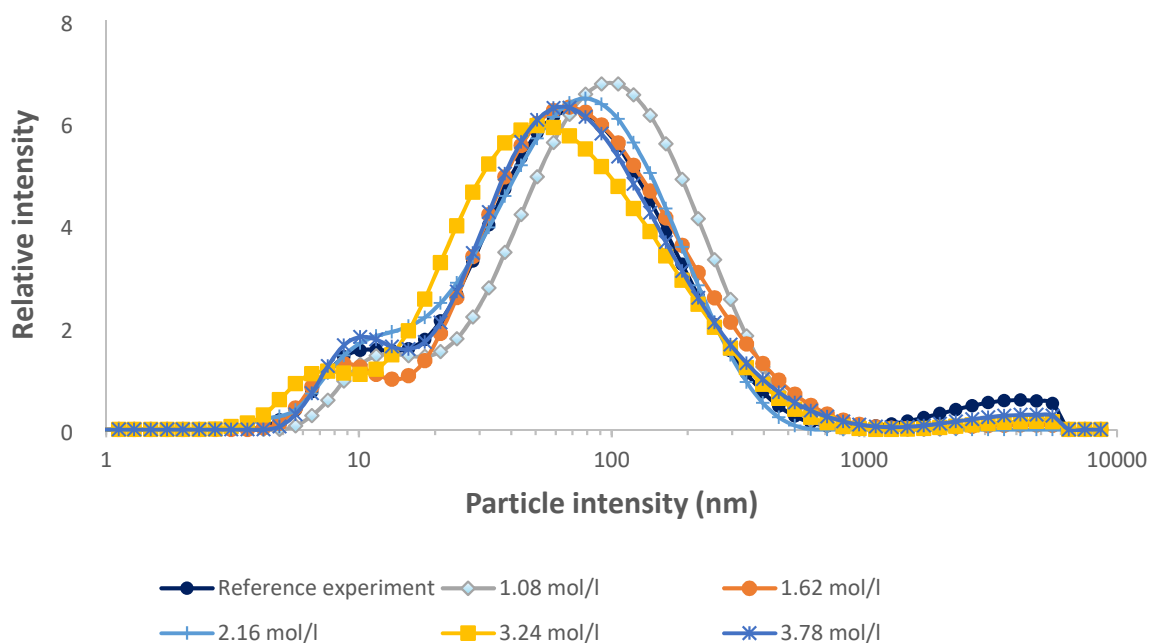


**Figure 17.** DLS measurement of the sols obtained as a function of styrene concentration. Measured on a Malvern Zetasizer Nanoseries.

The RAFT agent concentration and TsOH concentrations (1:1 ratio) were varied in unison. Experiments with 60, 80, 120 and 140% of the original CTA concentrations were conducted (Table S12). The expected decrease in  $M_n$  with increase in [RAFT] is seen.

**Table S12.** Effect of variation of the RAFT agent concentration <sup>a</sup>

[RAFT] M	% Conversion	$M_n^{\text{th}b}$ g mol <sup>-1</sup>	$M_n$	$\bar{D}$	$L^c$	$f^d$
0.00612	98	45200	39500	1.54	0.87	0.08
0.00816	97	33600	32000	1.48	0.95	0.04
0.0102	97	26900	22400	1.48	0.83	0.19
0.01224	99	22900	21200	1.50	0.92	0.09
0.0153	99	18400	12000	1.41	0.64	0.78

<sup>a</sup> Other conditions same as for reference experiment (Table S7). <sup>b</sup> Theoretical molar mass ( $M_n^{\text{th}}$ ) calculated using equation 3. <sup>c</sup> Fraction of living chains ( $L$ ) calculated using equation 6. <sup>d</sup> Initiator efficiency ( $f$ ) calculated using equation 4.

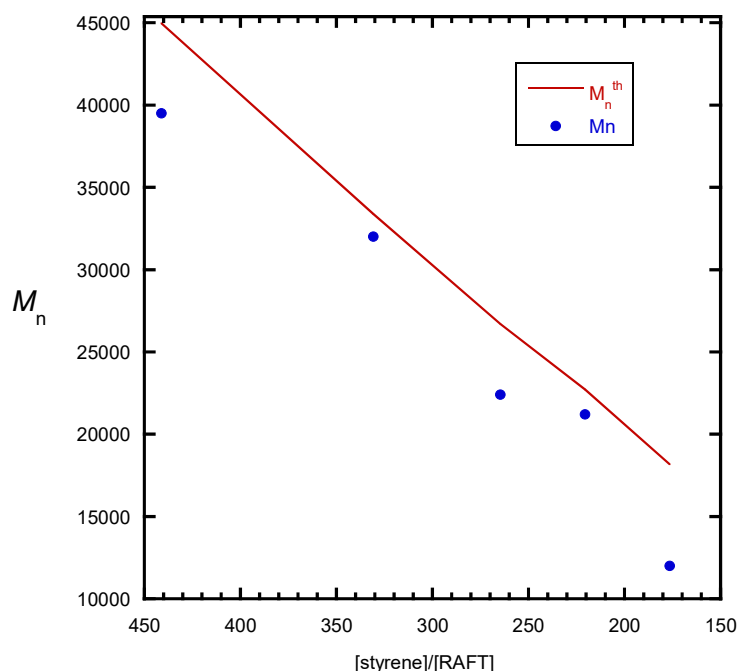


**Figure 18.** Theoretical and experimental  $M_n$  as a function of  $[\text{styrene}]/[1]$  for varying [RAFT]. Theoretical molar mass ( $M_n^{\text{th}}$ ) was calculated using equation 3.

### Chemspeed experiments with 4- (((cyanomethyl)thio)carbonothioyl)(methyl)amino)-1-methylpyridin-1-ium iodide (5).

All experiments with **5** gave polymers with multimodal distributions, which generally comprised a higher molar mass broader peak, a lower molar mass peak with a very sharp high tailing edge, and usually a series broad multimodal peaks at low molar mass. The  $M_n$  values listed below do not include these low molar mass peaks. GPC with UV detection shows that the broader peak at higher molar mass does not contain the thiocarbonylthio chromophore and the peaks at low molar mass contains little of this chromophore as was found for the Schlenk tube experiments (*vide infra*). Monomer conversions were very high in all experiments. A summary of Experiments where the concentrations of styrene and **5** were varied are presented below (Table S13 and Table S14, respectively).

Experiments were also conducted with in which SDS, ACPA, styrene and **3** were varied independently (Table S6).

**Table S13.** Effect of variation of the styrene concentration <sup>a</sup>

[Styrene] M	% Conversion	$M_n^{th,b}$ g mol <sup>-1</sup>	$M_p$ sharp	$M_p$ broad	$M_n$	$\mathcal{D}$
1.08	100	11000	7367	17000	5229	1.72
1.62	100	16500	19400	34400	11700	1.80
2.16	99	21800	26700	39300	-	-
2.70	100	27500	27800	36300	21143	1.30
3.24	100	33000	50200	27500	19900	1.63
3.78	100	38500	51400	29600	18100	1.78

<sup>a</sup> Other conditions same as for reference experiment (Table S7). <sup>b</sup> Theoretical molar mass ( $M_n^{th}$ ) calculated using equation 3.

**Table S14.** Effect of variation of the RAFT agent concentration <sup>a</sup>

[RAFT] M	% Conversion	$M_n^{th,b}$ g mol <sup>-1</sup>	$M_p$ sharp	$M_p$ broad	$M_n$	$\mathcal{D}$
0.0051	99	54500	24300	75800	24500	2.70
0.0102	100	27500	27800	36300	21143	1.30
0.0153	100	18400	27200	44200	11500	2.12
0.0204	99	13600	10900	30900	4850	2.41

<sup>a</sup> Other conditions same as for reference experiment (Table S7). <sup>b</sup> Theoretical molar mass ( $M_n^{th}$ ) calculated using equation 3.

- Chiefari, J.; Mayadunne, R. T. A.; Moad, C. L.; Moad, G.; Rizzardo, E.; Postma, A.; Skidmore, M. A.; Thang, S. H., Thiocarbonylthio Compounds (S:C(Z)S-R) in Free Radical Polymerization with Reversible Addition-Fragmentation Chain Transfer (RAFT Polymerization). Effect of the Activating Group Z. *Macromolecules* **2003**, *36* (7), 2273-2283.
- Moad, G.; Rizzardo, E.; Thang, S. H., Living Radical Polymerization by the RAFT Process. *Aust. J. Chem.* **2005**, *58*, 379-410.
- Zhou, Y.; Zhang, Z.; Postma, A.; Moad, G., Kinetics and mechanism for thermal and photochemical decomposition of 4,4'-azobis(4-cyanopentanoic acid) in aqueous media. *Polym. Chem.* **2019**, *10* (24), 3284-3287.